Measurement of Simplified Single- and Three-Phase Parameters for Harmonic Emission Assessment Based on IEEE 1459-2010

Giovanni Artale, *Member, IEEE*, Giuseppe Caravello, Antonio Cataliotti, *Member, IEEE*, Valentina Cosentino, *Member, IEEE*, Dario Di Cara, *Member, IEEE*, Salvatore Guaiana, Nicola Panzavecchia, *Senior Member, IEEE*, and Giovanni Tinè, *Member, IEEE*

***Abstract*— This article investigates the feasibility of using a simplified approach, based on the measurement of power ratio parameters, for harmonic emissions assessment at the point of common coupling (PCC). The proposed approach comes from the common concept of power factor correction and the definitions of the IEEE Std. 1459-2010, where line utilization and harmonic pollution levels are evaluated by means of ratios between the power quantities of the apparent power decomposition. In addition to the IEEE Std. 1459-2010 indicators, in this article, the behavior is studied of additional parameters that are conceptually similar to those defined by the IEEE Std. 1459-2010. The suitability of such parameters is discussed, for both single- and three-phase balanced/unbalanced cases, taking into account both their behavior in different scenarios and their effectiveness when the measurement uncertainty is taken into account. The study is supported by some simulation results that have been obtained on an IEEE benchmark power system, which allows reproducing linear and nonlinear load conditions, balanced and unbalanced operating conditions, and the presence of capacitors for power factor correction.**

***Index Terms*— Harmonic distortion, harmonic emission, IEEE Std. 1459-2010, power definitions, power measurement, power quality.**

I. Introduction

THE effective assessment of harmonic emissions and the detection of harmonic sources have been discussed for many years in the scientific literature. Several methodologies have been proposed, aimed at determining distortion contributions at both the utility and customer side of the point of common coupling (PCC). The issue is very important since it is at the basis of any billing strategy aimed at promoting users' participation to harmonic pollution reduction and power quality levels' improvement [1], [2]. From the perspective of the large-scale application of such methodologies, a very important aspect is related to the ease of implementation on smart meters (SMs) platforms, as well as on other typical measurement instruments, such as power quality analyzers (PQAs) and other intelligent electronic devices (IEDs). In fact, these instruments are widespread used in distribution grids both at the substation level and the customer side for energy billing and grid monitoring [3], [4]. Thus, they could also integrate simple metrics for harmonic emission assessment, without the need of installing new metering equipment in the power grid.

Voltage and current total harmonic distortion factors (THD_V and THD_I, respectively) are the most known indicators for the assessment of harmonic distortion. They are able to quantify the total amount of distortion; however, they cannot give information about the source of pollution. For this last purpose, several approaches have been studied for assessing harmonic emission levels and locating harmonic sources; such methods have been based on both distributed measurements and single-point measurement at PCC [5]–[14]. From the customer viewpoint, single-point measurements are more suitable since they can allow users to easily obtain information about the harmonic emission level and to be aware of the impact of harmonics at the delivery point. On the other hand, distributed measurements' strategies are more suitable for the distribution system operator (DSO) who can collect measurements coming for different points of the network. This can allow DSO to achieve more complete information about the harmonic state of the power grid and to separate customers' contributions to harmonic pollution in a given PCC from distortion coming from the grid.

As regards the standards' requirements, reference is currently made only to measurements of harmonic distortion levels, in terms of amplitudes of single harmonic components or THD values [15]–[17]. The measurement of electric power quantities in sinusoidal or distorted conditions, in both balanced or unbalanced situations, is covered by the IEEE Standard 1459-2010 [18]. It introduces some definitions of active, nonactive, and apparent powers, together with some indicators for harmonic pollution, line utilization, and load unbalance assessment (see Tables I and II). Such indicators are

Manuscript received July 22, 2020; revised October 8, 2020; accepted October 26, 2020. Date of publication November 16, 2020; date of current version January 6, 2021. This work was supported by the Grant PO FESR Sicilia 2014-2020, Action 1.1.5, Project n. 08000PA90246, project title: Smart grids per le Isole Minori (Smart Grids for Small Islands): I-Sole CUP G99J18000540007. The Associate Editor coordinating the review process was Seyed Hossein H. Sadeghi. *(Corresponding author: Valentina Cosentino.)*

Giovanni Artale, Giuseppe Caravello, Antonio Cataliotti, and Valentina Cosentino are with the Department of Engineering, Università di Palermo, 90128 Palermo, Italy (e-mail: giovanni.artale@unipa.it; giuseppe.caravello02@unipa.it; antonio.cataliotti@unipa.it; valentina.cosentino@unipa.it).

Dario Di Cara, Salvatore Guaiana, Nicola Panzavecchia, and Giovanni Tinè are with the Institute of Marine Engineering (INM), National Research Council (CNR), 90146 Palermo, Italy (e-mail: dario.dicara@cnr.it; nicola.panzavecchia@cnr.it; giovanni.tine@cnr.it).

Digital Object Identifier 10.1109/TIM.2020.3037949

TABLE I

IEEE STD 1459-2010 APPARENT POWER RESOLUTION—SINGLE-PHASE CASE

Power quantities	Combined	Fundamental	Nonfundamental	Apparent power resolution scheme	Indicators
Apparent [VA]	$S = V\,I$	$S_1 = V_1\,I_1$	$S_n = \sqrt{S^2 - S_1^2}$ $S_H = V_H\,I_H$	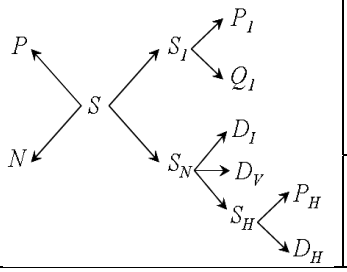	Line utilization $PF = P/S$ $PF_1 = P_1/S_1$
Active [W]	$P = \sum_{h=1}^{n} V_h I_h \cos\theta_h$	$P_1 = V_1 I_1 \cos\theta_1$	$P_h = \sum_{h\neq 1} V_h I_h \cos\theta_h = P - P_1$		
Nonactive [VAR]	$N = \sqrt{S^2 - P^2}$	$Q_1 = V_1 I_1 \sin\theta_1$	$D_I = V_1\,I_H$ $D_V = V_H\,I_1$ $D_H = \sqrt{S_H^2 - P_H^2}$		Harmonic pollution S_N/S_1

V_h and I_h are the rms values of the harmonic components of voltage and current, θ_h is their displacement and h is the harmonic order.

TABLE II

IEEE STD 1459-2010 EFFECTIVE APPARENT POWER RESOLUTION—THREE-PHASE CASE

Power quantities	Combined	Fundamental	Nonfundamental	Effective apparent power resolution scheme	Indicators
Apparent [VA]	$S_e = 3\,V_e\,I_e$	$S_{e1} = 3\,V_{e1}\,I_{e1}$, $S_1^+ = 3\,V_1^+\,I_1^+$ $S_{U1} = \sqrt{S_{e1}^2 - S_1^{+2}}$	$S_{eN} = \sqrt{S_e^2 - S_{e1}^2}$ $S_{eH} = 3\,V_{eH}\,I_{eH}$,	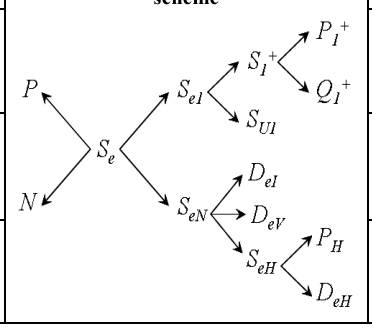	Line utilization $PF = P/S_e$ $PF_1^+ = P_1^+/S_1^+$
Active [W]	$P = \sum_{a,b,c}\sum_{h=1}^{n} V_h I_h \cos\theta_h$	$P_1^+ = 3\,V_1^+\,I_1^+ \cos\theta_1^+$	$P_H = \sum_{a,b,c}\sum_{h=2}^{n} V_h I_h \cos\theta_h = P - P_1$		Harmonic pollution S_{eN}/S_{e1}
Nonactive [VAR]	$N = \sqrt{S_e^2 - P^2}$	$Q_1^+ = 3\,V_1^+\,I_1^+ \sin\theta_1^+$	$D_{e1} = 3\,V_{e1}\,I_{eH}$ $De_V = 3\,V_{eH}\,I_{e1}$ $D_{eH} = \sqrt{S_{eH}^2 - P_H^2}$		Load unbalance S_{U1}/S_1^+

V_e, V_{e1}, V_{eH}, are the rms values of effective voltages; I_e, I_{e1}, I_{eH}, are the rms values of effective currents (total, fundamental, harmonic)

defined as ratios between the power quantities, recalling the common concept of power factor normally used for reactive power compensation. Customers are very familiar with this approach; therefore, the opportunity to implement a similar strategy also for harmonic pollution assessment and mitigation could be very useful. Furthermore, the measurement of IEEE 1459 power quantities is very simple since they are based on the separation of the fundamental components from the remaining harmonic content of voltage and current. Many commercial instruments (PQAs, SMs, and so on) already allow measuring fundamental and total active, nonactive, and apparent powers; starting from this, the measurement of power ratio indicators could be implemented very easily. The approach of assessing harmonic distortion level by means of power ratio parameters has been also proposed in the literature; for example, in [19] and [20], active and reactive power distortion factors have been introduced. Their formulation is similar to that of the IEEE 1459 indicators; in fact, they are expressed as ratios between harmonic and fundamental components of active and reactive powers.

In this framework, Cataliotti *et al.* [21] presented a preliminary study focused on the feasibility of using the IEEE 1459 indicators and new power ratio parameters for assessing harmonic emission levels at PCC. The study was based on the IEEE 1459 approach and the common concept of power factor correction. More in detail, in addition to the IEEE 1459 indicators, further parameters were introduced for harmonic emission assessment. They are meant to be used for harmonic mitigation purposes, with a similar approach to that of typical power factor correction. Artale *et al.* [22] presented an experimental study on the measurement uncertainty evaluation for both IEEE 1459 indicators and the new parameters in the single-phase case. They were measured with a single-phase PC-based sampling wattmeter (PC-SW) built with commercial data acquisition boards. This study was carried out in order to analyze the uncertainty on power ratios measurement, taking into account the PC-SW accuracy specifications and the correlation between the considered power quantities. The obtained results showed that the new indicators can be measured more accurately than the IEEE 1459 indicator for harmonic pollution assessment [22].

Starting from the results of [22], in this article, an extended study is presented on the measurement of the considered power ratios in both single- and three-phase sinusoidal, nonsinusoidal, balanced, and unbalanced cases. For the single- and three-phase balanced cases, the main findings of [21] and [22] are summarized, and new results are presented and discussed. For the three-phase unbalanced case, further indicators are introduced for both harmonic and unbalance assessments that are meant to be exploited with the same approach used for the balanced case.

This article is organized as follows. Section II describes the proposed indicators, in both single- and three-phase balanced and unbalanced cases. Section III presents some experimental results obtained in the laboratory setup with the single-phase PC-SW of [22] and some simulation results on a

standard IEEE three-phase test system in both sinusoidal, nonsinusoidal, balanced, and unbalanced conditions. Section IV presents the uncertainty evaluation on the measurement of the three-phase indicators; it is carried out by means of a Monte Carlo method and considering the accuracy specifications of measurement instrumentation and transducers typically used in distribution grids.

II. Proposed Distortion and Unbalance Indicators

A. Single-Phase Case

Following the approach of the IEEE 1459, the separation of fundamental components of power (active, reactive, and apparent) from the rest of the apparent power resolution terms allows introducing the parameters for line utilization and harmonic pollution assessment. The IEEE 1459 indicators for the line utilization are fundamental and total power factors, PF_1 and PF, respectively. In sinusoidal conditions, $\mathrm{PF}_1 = \mathrm{PF}$; this is the parameter commonly used for reactive power compensation, typically by means of capacitors banks. In ideal conditions, $\mathrm{PF}_1 = \mathrm{PF} = 1$. On the other hand, in the presence of harmonics, $\mathrm{PF}_1 \neq \mathrm{PF}$. To quantify the harmonic pollution, the IEEE 1459 introduces the ratio S_N/S_1, whose behavior is opposite to that of power factors, i.e., in ideal conditions (purely sinusoidal), $S_N/S_1 = 0$. This is true also for other power ratio parameters, such as active and reactive power distortion factors discussed in [19], whose value in the absence of harmonics is zero.

From the measurement viewpoint, all the IEEE 1459 parameters are very simple to be measured, and their measurement can be easily integrated into commercial instrumentation and used for line utilization improvement and harmonic pollution reduction. This is already made for power factor correction; a threshold is normally defined by the DSO, typically near 1, and the comparison between such threshold and the power factor determines the payment of a fee for reactive power absorption. To avoid such a fee, users are encouraged to provide reactive power compensation. On the other hand, similar policies for harmonic emission assessment and billing are not yet implemented. In this viewpoint, S_N/S_1 approaches zero in ideal conditions, and this can introduce some problems on measurement accuracy. In fact, in analogy with power factor correction, a threshold near to zero should be used for reference for harmonic billing and mitigation purposes; to compare the indicator with such threshold, very small values of S_N/S_1 should be measured, with a consequent increase of measurement uncertainty [22].

To avoid these limitations, in [21] and [22], the feasibility of some new indicators was initially investigated, with the aim of replacing the S_N/S_1 indicator of the IEEE 1459 with one or more parameters conceptually similar to the power factors, i.e., approaching 1 in ideal conditions. Such parameters were expressed as a function of the IEEE 1459 power quantities, in order to keep the advantage of easy implementation in practical measuring instruments (even in existing PQAs and SMs). More in detail, the considered power ratio parameters are P_1/S, S_1/S, and Q_1/N.

P_1/S can represent an indicator of the total line utilization amount, taking into account both the fundamental power and the harmonic distortion (which is included in S); in the sinusoidal case, $P_1/S = \mathrm{PF}_1 = \mathrm{PF}$, all approaching 1 in optimal line utilization condition. In real situations, $P_1/S < \mathrm{PF}_1$; the difference between indicators depends on the distortion amount.

S_1/S can allow quantifying the whole harmonic distortion level, considering both active and reactive powers; in the absence of harmonics, $S_1/S = 1$, and thus, the indicator behaves like power factors (i.e., it approaches 1 in ideal conditions). In this viewpoint, it can be seen as an indicator complimentary to S_N/S_1; it can provide the same information on the harmonic pollution level, but it can be measured more accurately than S_N/S_1 [22] and a threshold approach can be implemented, similar to that used for power factor correction.

Q_1/N represents an indicator of nonactive power components impact and pollution level. In earlier works, the authors studied the behavior of nonactive powers in distorted conditions, showing that it can be related to the load condition (linear or not) [13], [14]. In sinusoidal conditions, $Q_1 = N$ and $Q_1/N = 1$; thus, this indicator behaves as power factors, approaching 1 when the system tends to be purely sinusoidal. On the other hand, when harmonics are present, N increases with respect to Q_1 (since it includes all nonactive power components); thus, the indicator decreases. Also, for this indicator, a threshold approach can be implemented, similar to that used for power factor correction; furthermore, it can be measured more accurately than S_N/S_1 [22].

B. Three-Phase Balanced and Unbalanced Cases

In three-phase systems, the IEEE 1459 introduces the effective apparent power resolution, which allows dealing with sinusoidal, distorted, balanced, and unbalanced situations. In balanced conditions, the effective apparent power resolution leads to the same results of summing the phase power quantities. In this viewpoint, when the power system is balanced, the same indicators introduced for the single-phase case can be defined, and the power terms can be evaluated as the sum of the related phase (*a, b,* and *c*) quantities. Thus, for the IEEE 1459 indicators, the power ratios can be evaluated with an "arithmetic approach"

$$\mathrm{PF}_1 = \frac{P_1}{S_1} = \frac{P_{1a} + P_{1b} + P_{1c}}{S_{1a} + S_{1b} + S_{1c}} \tag{1}$$

$$\mathrm{PF} = \frac{P}{S} = \frac{P_a + P_b + P_c}{S_a + S_b + S_c} \tag{2}$$

$$\frac{S_N}{S_1} = \frac{S_{Na} + S_{Nb} + S_{Nc}}{S_{1a} + S_{1b} + S_{1c}}. \tag{3}$$

Similarly, for the newly defined power ratio indicators, the three-phase arithmetic formulation leads to the following expressions:

$$\frac{P_1}{S} = \frac{P_{1a} + P_{1b} + P_{1c}}{S_a + S_b + S_c} \tag{4}$$

$$\frac{S_1}{S} = \frac{S_{1a} + S_{1b} + S_{1c}}{S_a + S_b + S_c} \tag{5}$$

$$\frac{Q_1}{N} = \frac{Q_{1a} + Q_{1b} + Q_{1c}}{N_a + N_b + N_c}. \tag{6}$$

It should be noticed that many commercial instruments already implement the measurement of fundamental and total power quantities; thus, the measurement of the arithmetic power ratio indicators could be implemented without any difficulties or relevant computational burden increase.

On the other hand, in unbalanced conditions, the effective apparent power resolution leads to different results than those of the arithmetic approach. In this case, the arithmetic power ratio indicators can be still evaluated, but they will be different from those obtained by means of effective apparent power resolution. The indicators based on the "effective approach" are as follows.

1) $PF_1^+ = P_1^+/S_1^+$, $PF = P/S_e$, and S_{eN}/S_{e1} (IEEE 1459).
2) P_1^+/S_e, S_{e1}/S_e, and Q_1^+/N (new power ratio indicators for the unbalanced case).

In the IEEE 1459 approach, the fundamental positive sequence power factor PF_1^+ allows evaluating the positive-sequence power flow condition, i.e., the condition where only the power components of the ideal sinusoidal and balanced case are considered; PF and S_{eN}/S_{e1} allow evaluating the whole line utilization and harmonic pollution. As for the single-phase case, the IEEE 1459 parameter S_{eN}/S_{e1} approaches zero in the absence of distortion. On the other hand, in sinusoidal (and balanced) conditions, the new power ratio indicators approach the value of 1. Thus, they represent a more suitable alternative from the measurement viewpoint.

A further IEEE 1459 parameter is the ratio S_{U1}/S_1^+; it quantifies the load unbalance degree. In the absence of unbalance, $S_{U1}/S_1^+ = 0$, and the effective apparent power decomposition becomes analogous to that of the three-phase arithmetic approach. On the other hand, a complimentary new power ratio indicator can be introduced, i.e., S_1^+/S_{e1}; it approaches 1 in the absence of unbalance.

III. Indicators Characterization Simulation and Experimental Results

The effectiveness of the new indicators versus the IEEE 1459 ones has been preliminarily verified in [21], in both single- and three-phase balanced cases. In summary, for the single-phase case, a simple test system was simulated; it was able to reproduce different situations, where the supply and/or the load can be responsible for the harmonic distortion. A capacitor for power factor correction was also added at the load side in order to investigate how it can worsen the harmonic pollution level at the PCC. Similarly, the three-phase test system used in [21] allowed simulating different situations, with both sinusoidal or distorted supply, one linear load (with or without capacitor banks for power factor correction), and a nonlinear load. The obtained results provided a first confirmation of the feasibility of using the new power ratios for the harmonic emission level assessment at the PCC. On the other hand in [22], some results have been presented on the evaluation of uncertainty on the measurement of the considered indicators. It was shown that the measurement of the new indicators can be more accurate than that of the IEEE Std. 1459 indicator for harmonic pollution assessment.

In the following, further results are presented in both single- and three-phase unbalanced cases, showing the behavior of considered indicators in different simulated and experimental conditions. In a three-phase case, indicators of both arithmetic approach and the one based on effective apparent power resolution are evaluated and compared.

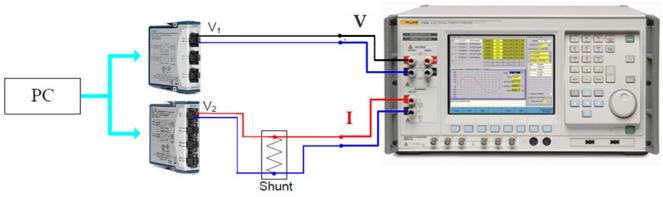

Fig. 1. Experimental single-phase test bench.

A. Single-Phase Case Experimental Results

The single-phase study was carried out experimentally, by means of the test bench presented in [22]. A PC-SW was used for measurements; test voltage and currents were generated by means of a calibrator Fluke Electrical Power Standard 6100A (see Fig. 1). PC-SW voltage channel was built with a data acquisition board NI USB 9225; the current channel included both the data acquisition board NI USB 9239 and a current shunt Fluke A40B. For the tests, a sampling frequency was set to 50 kS/(with simultaneous sampling on the two PC-SW channels).

In order to analyze the indicators' behavior in different operating conditions, various tests were made, by changing both amplitudes and phases of voltage and current harmonics. For each test condition, 1000 trials were repeated, and measurements' results were collected. The correlations among each pair of power quantities involved in power ratio indicators were evaluated. Then, measurement uncertainty was evaluated according to the procedure described in [22].

For example, Figs. 2 and 3 and Table III report the results obtained in the test condition with a fundamental and a fifth-harmonic component on both voltage and current. According to standards on electricity metering equipment for active and reactive energies, amplitudes of harmonic voltage and current were set to 10% and 40% of the fundamental component, respectively (V = 230 V and I = 5 A); phase shift between the fundamental voltage and current was set equal to 30°; and phase shift between harmonic voltage and current was changed between −90° and +90°.

As an example, some results of the correlation analysis for one test are reported in Fig. 2. For this test, the comparison between IEEE 1459 indicators and the proposed indicators is reported in Table III. (comparison of mean values, uncertainties, and correlation coefficients). The indicators results obtained by varying the phase shift between harmonic voltage and current are reported in Fig. 3.

As shown also in [22], in all tests, the lowest correlation has been observed between S_N and S_1; this, together with the small value of the ratio between these powers, contributes to higher uncertainty on the measurement of the IEEE 1459 indicator S_N/S_1. On the contrary, the strongest correlation has been observed between the pairs (S_1, S) and (Q_1, N); this contributes to achieving a lower uncertainty on the measurement of the newly defined indicators (S_1/S) and (Q_1/N).

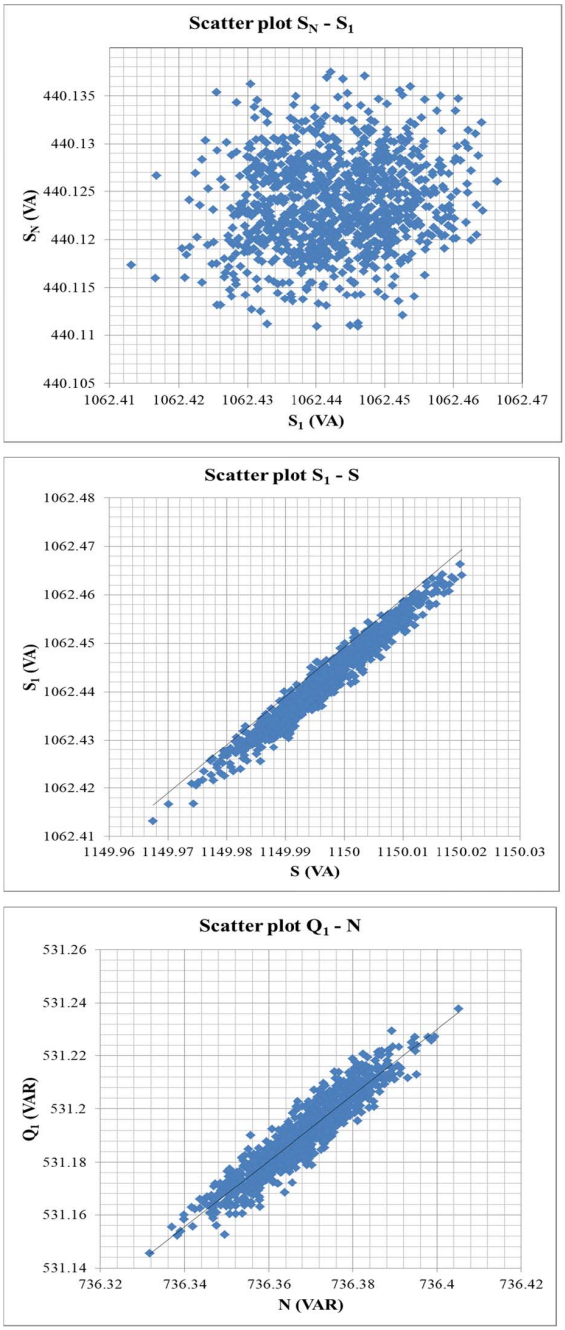

Fig. 2. Results of correlation analysis. Scatter plots of powers pairs (S_N-S_1, S_1-S, and Q_1-N). Experimental test with fifth harmonic on both voltage and current; 30° phase shift between both fundamental and harmonic components.

Measurement uncertainties of power ratios S_1/S and Q_1/N were always significantly lower than that of S_N/S_1; worst case values were under 300 ppm for S_1/S, under 700 ppm for Q_1/N, and over 4000 ppm for S_N/S_1. In the tests with different phase shifts between voltage and current harmonics, Q_1/N showed the most significant changes (see Fig. 3).

B. Three-Phase Distorted and Unbalanced Case Simulation Results

The three-phase simulation study was carried out on the IEEE Test System n. 2 [23]. This is an MV radial distribution network, with typical residential and industrial loads and

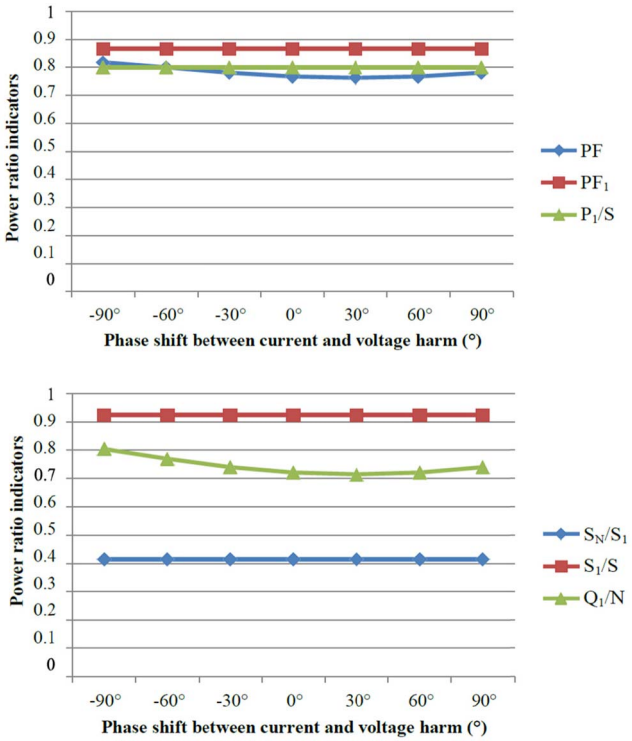

Fig. 3. Results of indicators. Experimental test with the fifth harmonic on both voltage and current; 30° phase shift between both fundamental and harmonic components; and phase shift between harmonic components from −90° to +90°.

TABLE III

MEAN VALUES AND UNCERTAINTIES OF POWER RATIO INDICATORS AND CORRELATION COEFFICIENTS OF POWERS PAIRS. EXPERIMENTAL TEST CONDITION OF FIG. 2

IEEE Std. 1459 Indicators	*Indicators mean values*	*PF*	PF_1	S_N/S_1
		0.768	0.866	0.414
	Correlation coefficients	*r(P, S)*	$r(P_1, S_1)$	$r(S_N, S_1)$
		0.713	0.745	0.141
	Uncertainties [ppm]	$\dot{u}_{PF}$	$\dot{u}_{PF1}$	$\dot{u}_{Sn/S1}$
		239	231	1027
New indicators	*Indicators mean values*	P_1/S	S_1/S	Q_1/N
		0.800	0.924	0.721
	Correlation coefficients	$r(P_1, S)$	$r(S_1, S)$	$r(Q_1, N)$
		0.726	0.978	0.935
	Uncertainties [ppm]	$\dot{u}_{P1/S}$	$\dot{u}_{S1/S}$	$\dot{u}_{Q1/N}$
		234	227	497

equipment (linear *RL* loads, fluorescent light banks, adjustable speed drives, voltage regulators, shunt capacitors, and so on). Simplified schemes of the test system are reported in Fig. 4. Complete network and loads' data are given in [23].

In this study, loads have been aggregated, obtaining a simplified power system with a power source (at node 50), two PCC (PCC1 and PCC2), and five aggregated loads [13].

1) PCC1 is at node 32; the loads connected to PCC1 are as follows:
   a) L1 (power transformer at node 33 with single-phase load at node 34; no shunt capacitors);
   b) L2 (single-phase load at node 45, phase-phase load at node 46, and half the distributed load between nodes 32 and 71; no shunt capacitors).

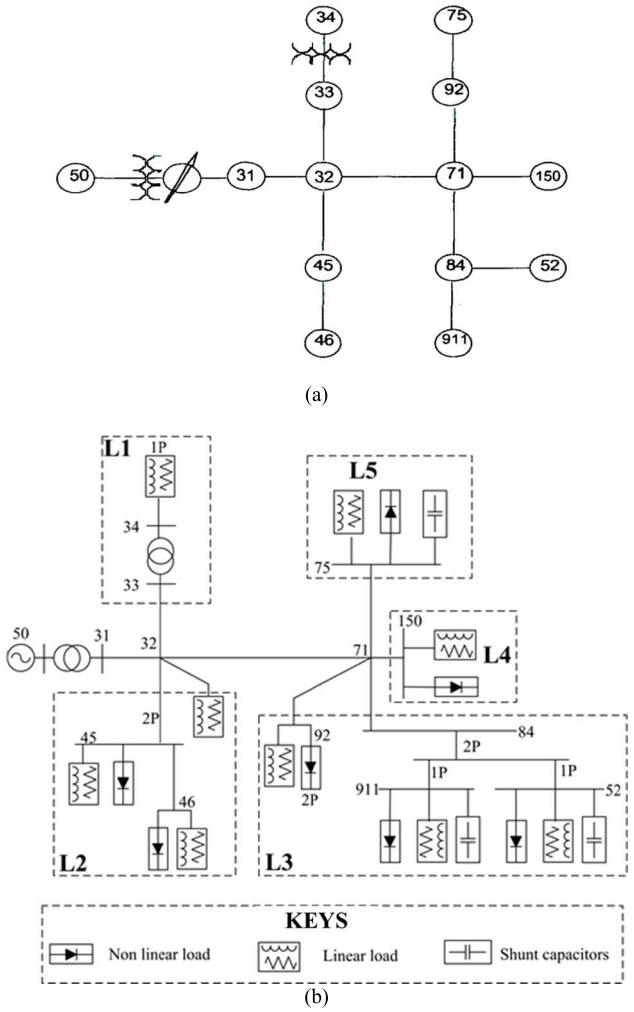

Fig. 4. IEEE Test System. (a) Original scheme [23]. (b) Scheme with aggregated loads [13].

2) PCC2 is at node 71; the loads connected to PCC2 are as follows:
   a) L3 (half the distributed load between nodes 32 and 71, and phase-phase load at node 92; single-phase loads at nodes 52 and 911 with shunt capacitors);
   b) L4 (three-phase load at node 150);
   c) L5 (three-phase load at node 75, with shunt capacitors).

Main loads characteristics in terms of load type and injected harmonics are summarized in Table IV and Table V. Table VI reports THD and unbalance degrees for both voltages and currents for the five aggregated loads.

This test system has been developed for unbalanced harmonics propagation studies. In this work, it allowed evaluating the suitability of the two proposed sets of three-phase indicators (both those based on the arithmetic approach and those based on an effective approach), whose behavior can be different in the presence of unbalance. The test system does not take into account the presence of interharmonics, even if they can be present in real power systems. With respect to this, the proposed indicators should not be affected by interharmonics, as they are based on the separation of the fundamental components from the remaining distortion content (including interharmonics, if any). On the other hand, interharmonics can have an impact on measurement accuracy (e.g., they can cause spectral interference phenomena or effect of fundamental and/or harmonic components fluctuations).

Different working conditions were simulated in the time domain, both in the original network configuration and by changing one or more loads. In more detail, to reproduce

TABLE IV
CURRENT SPECTRA OF HARMONIC LOADS

Harmonic order	Fluorescent Lamps (FL)		Adjustable speed Drives (ASD)		Other Loads	
	Amplitude [p.u.]	Phase [°]	Amplitude [p.u.]	Phase [°]	Amplitude [p.u.]	Phase [°]
1	1	-41.2	1	-1.5	1	-35
2	0	--	0	--	0	--
3	0.2	273.4	0.542	0.7	0.007	-105.8
4	0	--	0	--	0.095	-167.4
5	0.107	339	0.152	110.8	0.002	-275.5
6	0	--	0	--	0.083	-42.6
7	0.021	137.7	0.069	151.9	0	--
8	0	--	0	--	0.005	-247.8
9	0.014	263.2	0.043	-95	0	--
10	0	--	0	--	0	--
11	0.009	39.8	0.036	-13.9	0	--
12	0	--	0	--	0	--
13	0.006	182.4	0.029	95.2	0	--
14	0	--	0	--	0	--
15	0.005	287	0.025	-182.7	0	--

TABLE V
MAIN CHARACTERISTICS OF TEST SYSTEM LOADS

Aggr. load	Node	Phase A load powers (fundamental)		Phase B load powers (fundamental)		Phase C load powers (fundamental)	
		kW	kvar	kW	kvar	kW	kvar
L1	34	42.63	20.18				
		Harmonic loads: NO					
L2	45			170.53	125.09		
		Harmonic loads: YES (other, 60%)					
	46			230.22	131.97		
		Harmonic loads: YES (FL, 20%; ASD, 20%; other, 60%) Phase-phase load between phases B and C					
	32-71	8.24	4,72	33.20	19.03	58.48	48.52
		Harmonic loads: NO Half distributed load between nodes 32 and 71					
L3	52	127.90	85.79				
		Harmonic loads: YES (FL, 10%; ASD, 10%; other, 60%)					
	92					170.53	151.38
		Harmonic loads: YES (FL, 15%; ASD, 20%; other, 15%) Phase-phase load between phases C and A					
	911					170.53	80.74
		Harmonic loads: YES (FL, 15%; ASD, 20%; other, 15%) Shunt capacitors (100 kvar)					
	32-71	16.48	9.45	66.40	38.06	116.97	97.05
		Harmonic loads: NO Half distributed load between nodes 32 and 71					
L4	150	383.70	219.95	383.70	219.95	383.70	213.95
		Harmonic loads: YES (FL, 30%; other, 60%)					
L5	75	486.02	189.07	68.21	60.55	289.91	212.65
		Harmonic loads: YES (FL, 15%; ASD, 20%; other, 15%) Shunt capacitors (200 kvar for each phase)					

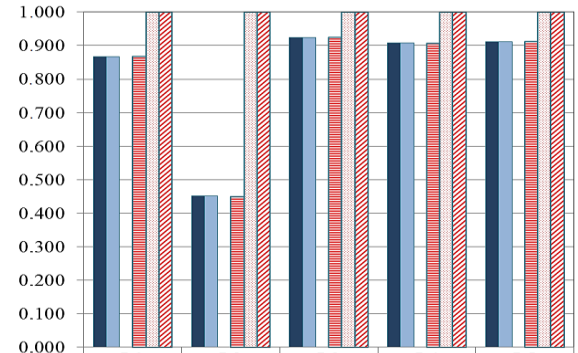

	L1	L2	L3	L4	L5
PF_1	0.868	0.451	0.925	0.908	0.912
PF	0.868	0.451	0.925	0.908	0.912
S_N/S_1	0.000	0.000	0.000	0.000	0.000
P_1/S	0.868	0.451	0.925	0.908	0.912
S_1/S	1.000	1.000	1.000	1.000	1.000
Q_1/N	1.000	1.000	1.000	1.000	1.000

Fig. 5. Simulation results of the power ratios in the case of all linear loads. Power ratios from the arithmetic approach.

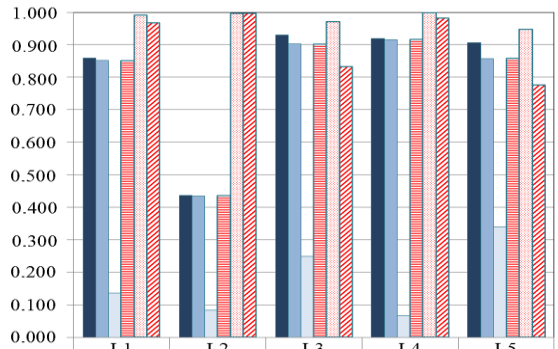

	L1	L2	L3	L4	L5
PF_1	0.859	0.437	0.929	0.919	0.907
PF	0.851	0.435	0.903	0.916	0.858
S_N/S_1	0.137	0.083	0.248	0.067	0.341
P_1/S	0.851	0.435	0.902	0.917	0.858
S_1/S	0.991	0.997	0.971	0.998	0.947
Q_1/N	0.968	0.996	0.833	0.981	0.777

Fig. 6. Simulation results of the proposed approach in the case of all nonlinear loads (original configuration). Power ratios from the arithmetic approach.

different loads configuration scenarios, some nonlinear and/or unbalanced loads were replaced by equivalent linear and balanced *RL* loads having the same power size and fundamental power factor of the original ones. For each scenario, the time-domain simulation of the test system was run; for each aggregated load, the samples of voltage and current waveforms were saved; then, they were processed to obtain the IEEE 1459 power quantities and the power ratio indicators.

For example, the results obtained for the network configuration with all linear loads are shown in Fig. 5. As expected, for all loads, PF_1 and PF are equal, and S_N/S_1 is zero. For loads L1 and L2, power factors are low because no shunt capacitors are connected to such loads. P_1/S is equal to PF_1, while S_1/S and Q_1/N are equal to 1.

The results obtained in the initial scenario, i.e., in the original network configuration, with all nonlinear/unbalanced loads are shown in Figs. 6 and 7. It can be observed that, for loads L1 and L2 at PCC1, where distortion levels are low, the values of S_1/S and Q_1/N are very near to 1, and P_1/S is almost equal to PF_1. On the other hand, for loads at PCC2, distortion levels are higher; for such loads S_1/S and even more, Q_1/N are lower than 1, and P_1/S is lower than PF_1. It can also be noted that the lowest values of S_1/S and Q_1/N are obtained for L3 and L5, where shunt capacitors are present. This is due to the fact that capacitors amplify the distortion at the metering section; thus, their effect on the considered indicators is similar to that of a nonlinear load. The same considerations can be made by considering the power ratios derived from the effective apparent power resolution (see Fig. 7). In this case, the high differences between PF_1^+, *PF*, and P_1^+/S_e are due to the presence of unbalance; the same is for S_{e1}/S_e and Q_1^+/N (in the figure, the unbalance amount is quantified by means of the new indicator S_1^+/S_{e1}). Finally, by comparing the results of Figs. 6 and 7, it can be observed that the power ratios obtained from the arithmetic approach are not affected by the presence of unbalance. This confirms that they could be used for harmonic emission assessment in both balanced and unbalanced situations.

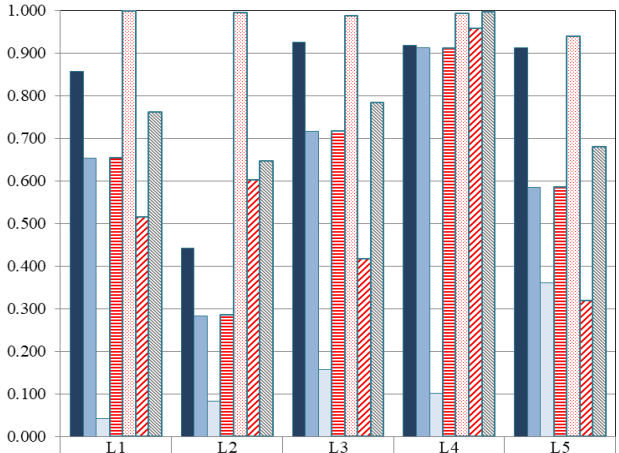

	L1	L2	L3	L4	L5
PF_1^+	0.859	0.443	0.927	0.919	0.914
PF	0.654	0.282	0.718	0.913	0.585
S_{eN}/S_{e1}	0.042	0.083	0.157	0.101	0.362
P_1^+/S_e	0.655	0.285	0.719	0.914	0.586
S_{e1}/S_e	0.999	0.997	0.988	0.995	0.940
Q_1^+/N	0.517	0.603	0.418	0.960	0.320
S_1^+/S_{e1}	0.763	0.647	0.785	0.999	0.682

Fig. 7. Simulation results of the proposed approach in the case of all nonlinear loads (original configuration). Power ratios from apparent power resolution.

IV. Measurement Uncertainty Evaluation

In order to evaluate the measurement uncertainty impact on power ratios, uncertainty propagation was studied starting from the measurement uncertainties of the IEEE 1459 power quantities. The study was carried out by considering the accuracy specifications of measurement instruments and transducers typically used in distribution networks, i.e., voltage and current electronic instrument transformers (VTs and CTs) and PQAs.

In more detail, PQAs were considered with an accuracy class of 0.5 and 2 for active and reactive power measurements, respectively, ($e_{\mathrm{PQA}_P} = 0.5\%$ and $e_{PQA_Q} = 2\%$), and 0.2 for voltage and current measurements ($e_{\mathrm{PQA}_V} = e_{\mathrm{PQA}_I} = 0.2\%$). VTs and CTs of class 0.2S were considered as measurement

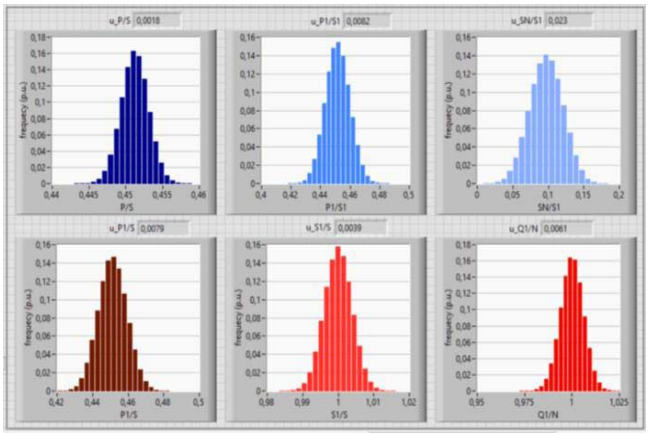

Fig. 8. Monte Carlo results in the case of all nonlinear loads (original configuration). Load L2.

TABLE VI

THD FACTORS AND UNBALANCE DEGREES. ORIGINAL NETWORK CONFIGURATION

PCC	Loads	THD_V[%] (mean value)	THD_I[%] (mean value)	Vi/Vd [%]	Ii/Id [%]
1	L1	4,4	2,16	0,33	84,6
	L2		6,42	0,33	95,6
2	L3	7,35	7,86	0,91	74,3
	L4		7,34	0,91	3,24
	L5		30,3	0,91	29,7

TABLE VII

RELATIVE UNCERTAINTIES OBTAINED IN THE CASE OF ALL NONLINEAR LOADS' ORIGINAL NETWORK CONFIGURATIONS

Loads	u_P/S	u_P_1/S1	u_S_N/S_1	u_P_1/S	u_S_1/S	u_Q_1/N
L1	0,29%	1,0%	24%	0,89%	0,45%	0,49%
L2	0,55%	2,2%	40%	2,1%	0,49%	0,11%
L3	0,28%	0,95%	12%	0,75%	0,46%	1,0%
L4	0,25%	0,82%	32%	0,63%	0,39%	0,32%
L5	0,26%	0,89%	5,0%	0,69%	0,42%	0,79%

transducers. According to the standard requirements [24], the maximum allowed ratio error and phase displacement for class 0.2S CTs are equal to $\eta_{CT} = \pm 0.2\%$ and $\varepsilon_{CT} = \pm 0.3$ crad, respectively, for currents between 20% and 120% of the CT rated current; for currents equal to 5% of the rated current, maximum ratio error and phase displacement allowable are $\eta_{CT} = \pm\ 0.35\%$ and $\varepsilon_{CT} = \pm\ 0.45$ crad, respectively; and for currents from 5% to 20% of the rated value, maximum allowable ratio error and phase displacement are calculated by means of a linear interpolation between the two reference limits. These limits are referred to as the rms value of the signal in sinusoidal conditions. For combined quantities, in the case of distorted signals, the standard [24] prescribes incrementing these limits by a 15% factor. On the other hand, for fundamental quantities standard, [24] prescribes the following allowable errors: $\eta_{CT1} = \pm 1\%$ and $\varepsilon_{CT1} = \pm\ 1.8$ crad. The same considerations can be applied to VTs.

Starting from the above-described error limits, the Monte Carlo simulations were performed by assuming uniform distribution for each of the abovementioned errors. In this case, the extremes of the uncertainty range are equal to the maximum errors reported above; 10^5 Monte Carlo iterations were performed. At each iteration, i, a random value, was chosen inside the uncertainty range for each of the considered uncertainty contributions. For example, fundamental voltage, current, and active power are obtained using the following equations [25]:

$$V_{1i} = \left(1 - \frac{\eta_{\mathrm{VT1i}}}{100}\right) \cdot \left(1 - \frac{e_{\mathrm{PQA}_{V1i}}}{100}\right) V_1 \tag{7}$$

$$I_{1i} = \left(1 - \frac{\eta_{\mathrm{CTi1}}}{100}\right) \cdot \left(1 - \frac{e_{\mathrm{PQA}_{Ii1}}}{100}\right) I_1 \tag{8}$$

$$P_{1_i} = \left(1 - \frac{\eta_{\mathrm{CT1}_i}}{100} - \mathrm{sen}\varepsilon_{\mathrm{CT1}_i} \cdot tg\varphi\right) \times \left(1 - \frac{\eta_{\mathrm{VT1}_i}}{100} + \mathrm{sen}\varepsilon_{\mathrm{VT1}_i} \cdot tg\varphi\right) \cdot \left(1 - \frac{e_{\mathrm{PQA}_{P1i}}}{100}\right) \cdot P_1 \tag{9}$$

where I_1, V_1, and P_1 are the values obtained in the simulation on the IEEE test system for a given working condition and a given node; V_{1i}, I_{1i}, and P_{1i} are the quantities obtained considering the uncertainty propagation on the measurement chain at i iteration.

The Monte Carlo simulations were performed both for the fundamental and the total quantities in order to obtain the uncertainties in both the power quantities of the IEEE 1459 apparent power resolution and the considered indicators for harmonic emission assessment.

As an example, the frequency distributions obtained with Monte Carlo simulations for load L2 are reported in Fig. 8, in the case of all nonlinear loads (original configuration). The uncertainties obtained in this test case for all loads are summarized in Table VII. As can be seen, the uncertainty obtained for the index S_N/S_1 is comparable to the parameter value (see Fig. 6). This means that measurement uncertainty can significantly affect the parameter, and the measured value can be not meant for practical applications. On the other hand, the new indicators, S_1/S and Q_1/N, have lower uncertainties, thus confirming their potentiality for a better harmonic emission assessment.

V. CONCLUSION

This work has been aimed at investigating the feasibility of using the IEEE Std. 1459-2010 power factors and other newly defined power ratio parameters for the assessment of harmonic emissions level at the PCC. A critical analysis has been made on measurement issues related to the evaluation of the IEEE 1459 parameters for line utilization and harmonic pollution parameters. To overcome some limitations of the IEEE 1459 indicators, new power ratios have been introduced and analyzed. They are conceptually similar to those defined by IEEE 1459, but they can be more accurately measured with instrumentation and transducers normally employed in distribution power grids. The suitability of the proposed parameters has been shown for both single- and three-phase balanced/unbalanced cases, by analyzing the indicators' behavior in different scenarios. Their effectiveness has been also discussed when measurement uncertainty is taken into account. The obtained results confirm that the proposed parameters have better behavior than the IEEE 1459 indicators

for harmonic pollution. Due to their simple formulation and the "power factor like" behavior, they are suitable for accurate measurements, and they could be easily integrated into common instrumentation for power system measurements and billing purposes.

The presented study also confirms that the presence of capacitor banks for power factor compensation can worsen the harmonic distortion levels. In fact, capacitors act almost as nonlinear loads, and they can produce harmonic resonance phenomena (as their impedance decreases when frequency increases). Therefore, it is important to evaluate the performance of methods for harmonic emission assessment also in the presence of capacitors. This is particularly true in the context of smart grids, where the presence of distributed generation, power electronic inverters, and nonlinear loads, combined with capacitor banks, may cause a significant increase in distortion levels. In this viewpoint, active filters and compensators can be more suitable for compensation purposes. With respect to this, the results shown in this article confirm the feasibility of the proposed approach based on power ratio indicators also in the presence of capacitors.

REFERENCES

[1] G. V. de Andrade Jr., S. R. Naidu, M. G. G. Neri, and E. G. da Costa, "Estimation of the utility's and consumer's contribution to harmonic distortion," *IEEE Trans. Instrum. Meas.*, vol. 58, no. 11, pp. 3817–3823, Nov. 2009.

[2] S. Vlahinic, D. Brnobic, and N. Stojkovic, "Indices for harmonic distortion monitoring of power distribution systems," *IEEE Trans. Instrum. Meas.*, vol. 58, no. 5, pp. 1771–1777, May 2009.

[3] H. Dirik, I. U. Duran, and C. Gezegin, "A computation and metering method for harmonic emissions of individual consumers," *IEEE Trans. Instrum. Meas.*, vol. 68, no. 2, pp. 412–420, Feb. 2019.

[4] D. Saxena, S. Bhaumik, and S. N. Singh, "Identification of multiple harmonic sources in power system using optimally placed voltage measurement devices," *IEEE Trans. Ind. Electron.*, vol. 61, no. 5, pp. 2483–2492, May 2014.

[5] C. Muscas, L. Peretto, S. Sulis, and R. Tinarelli, "Investigation on multipoint measurement techniques for PQ monitoring," *IEEE Trans. Instrum. Meas.*, vol. 55, no. 5, pp. 1684–1690, Oct. 2006.

[6] E. J. Davis, A. E. Emanuel, and D. J. Pileggi, "Evaluation of single-point measurements method for harmonic pollution cost allocation," *IEEE Trans. Power Del.*, vol. 15, no. 1, pp. 14–18, Jan. 2000.

[7] W. Xu and Y. Liu, "A method for determining customer and utility harmonic contributions at the point of common coupling," *IEEE Trans. Power Del.*, vol. 15, no. 2, pp. 804–811, Apr. 2000.

[8] K. Srinivasan, "On separating customer and supply side harmonic contributions," *IEEE Trans. Power Del.*, vol. 11, no. 2, pp. 1003–1012, Apr. 1996.

[9] T. Pfajfar, B. Blazic, and I. Papic, "Harmonic contributions evaluation with the harmonic current vector method," *IEEE Trans. Power Del.*, vol. 23, no. 1, pp. 425–433, Jan. 2008.

[10] Z. Staroszczyk, "A method for real-time, wide-band identification of the source impedance in power systems," *IEEE Trans. Instrum. Meas.*, vol. 54, no. 1, pp. 377–385, Feb. 2005.

[11] I. Urbina-Salas, J. R. Razo-Hernandez, D. Granados-Lieberman, M. Valtierra-Rodriguez, and J. E. Torres-Fernandez, "Instantaneous power quality indices based on single-sideband modulation and wavelet packet-Hilbert transform," *IEEE Trans. Instrum. Meas.*, vol. 66, no. 5, pp. 1021–1031, May 2017.

[12] D. Serfontein, J. Rens, G. Botha, and J. Desmet, "Continuous event-based harmonic impedance assessment using online measurements," *IEEE Trans. Instrum. Meas.*, vol. 65, no. 10, pp. 2214–2220, Oct. 2016.

[13] A. Cataliotti, V. Cosentino, and S. Nuccio, "Comparison of nonactive powers for the detection of dominant harmonic sources in power systems," *IEEE Trans. Instrum. Meas.*, vol. 57, no. 8, pp. 1554–1561, Aug. 2008.

[14] A. Cataliotti and V. Cosentino, "Disturbing load identification in power systems: A single-point time-domain method based on IEEE 1459-2000," *IEEE Trans. Instrum. Meas.*, vol. 58, no. 5, pp. 1436–1445, May 2009.

[15] *Testing and Measurement Techniques—Section 7: General Guide on Harmonics and Interharmonics Measurement and Instrumentation for Power Supply Systems and Equipment Connected Thereto*, Standard 61000-4-7, 2002.

[16] *Electromagnetic Compatibility (EMC)—Part 3-6: Limits—Assessment of Emission Limits for the Connection Of Distorting Installations to MV, HV and EHV Power Systems*, IEC TR Standard 61000-3-6, 2008.

[17] *Electromagnetic Compatibility (EMC)—Part 3-14: Assessment of Emission Limits for Harmonics, Interharmonics, Voltage Fluctuations and Unbalance for the Connection of Disturbing Installations to LV Power Systems*, IEC TR Standard 61000-3-14, 2011.

[18] *IEEE Standard Definitions for the Measurement of Electric Power Quantities Under Sinusoidal, Non Sinusoidal, Balanced or Unbalanced Conditions*, Standard 1459-2010, May 2010.

[19] S. Chattopadhyay, A. Chattopadhyaya, and S. Sengupta, "Harmonic power distortion measurement in park plane," *Measurement*, vol. 51, pp. 197–205, May 2014.

[20] S. Chattopadhyay, M. Mitra, and S. Sengupta, *Electric Power Quality*. New York, NY, USA: Springer, 2011, pp. 1–182.

[21] A. Cataliotti, V. Cosentino, D. Di Cara, and G. Tinè, "IEEE Standard 1459 power quantities ratio approaches for simplified harmonic emissions assessment," in *Proc. 18th Int. Conf. Harmon. Qual. Power (ICHQP)*, Ljubljana, Slovenia, May 2018, pp. 1–6.

[22] G. Artale *et al.*, "Measurement uncertainty of harmonic emission indicators based on IEEE Standard 1459-2010," in *Proc. IEEE Int. Instrum. Meas. Technol. Conf. (I2MTC)*, May 2020, pp. 1–6.

[23] R. Abu-Hashim *et al.*, "Test systems for harmonics modeling and simulation," *IEEE Trans. Power Del.*, vol. 14, no. 2, pp. 579–587, Apr. 1999.

[24] *Instrument Transformers—Part 8: Electronic Current Transformers*, Standard 60044-8, 2002.

[25] *Equipment for Measuring Electrical Energy (A.C.)—Guide to Component Selection, Installation And Verification, (Sistemi Di Misura Dell'Energia Elettrica (CA)—Guida Alla Composizione, Installazione E Verifica) in Italian*, document CEI 13-7, 2015.

Giovanni Artale (Member, IEEE) received the M.S. degree in electronic engineering and the Ph.D. degree in electronic and telecommunication engineering from the University of Palermo, Palermo, Italy, in 2010 and 2014, respectively.

He is currently a Research Collaborator with the Department of Engineering, University of Palermo. His current research interests include low-frequency harmonic analysis algorithms, power line communications, and smart grids.

Giuseppe Caravello received the M.S. degree in electrical engineering from the University of Palermo, Palermo, Italy, in 2018, where he is currently pursuing the Ph.D. degree in energy and ICT.

His research interests include power system measurement and monitoring, impacts of distributed generations on power systems, artificial intelligence, and energy storage systems.

Antonio Cataliotti (Member, IEEE) received the M.S. and Ph.D. degrees in electrical engineering from the University of Palermo, Palermo, Italy, in 1992 and 1998, respectively.

He is currently a Full Professor of electrical and electronic measurements with the Department of Engineering, University of Palermo. His current research interests include power quality measurements, power line communications, and smart grids.

Valentina Cosentino (Member, IEEE) received the M.S. and Ph.D. degrees in electrical engineering from the University of Palermo, Palermo, Italy, in 2001 and 2005, respectively.

She is currently an Associate Professor of electrical and electronic measurements with the Department of Engineering, University of Palermo. Her current research interests include energy and power quality measurements, detection of disturbances sources in power systems, virtual instrumentation, and smart grids.

Dario Di Cara (Member, IEEE) received the M.S. and Ph.D. degrees in electrical engineering from the University of Palermo, Palermo, Italy, in 2005 and 2009, respectively.

He is currently a Researcher with the Institute of Marine Engineering, Italian National Research Council, Palermo. His current research interests include power quality measurements, current transducers characterization in nonsinusoidal conditions, power line communications, and smart grids.

Salvatore Guaiana received the M.S. degree in electronics and photonics engineering and the Ph.D. degree in energy and information technologies from the University of Palermo, Palermo, Italy, in 2012 and 2019, respectively.

He is currently a Research Fellow with the Institute of Marine Engineering, Italian National Research Council, Palermo. His current research interests include power line communications, development of microcontroller systems, and communications protocols for smart grids applications.

Nicola Panzavecchia (Senior Member, IEEE) received the M.S. degree in computer science and the master's degree in domotics and building automation from the University of Palermo, Palermo, Italy, in 2007 and 2011, respectively.

Since 2007, he has been a consultant, a programmer, and a web system administrator. He is currently a Researcher with the Institute of Marine Engineering, Italian National Research Council, Palermo. His current research interests include software development for energy management and embedded systems, smart grids, and power line communications.

Giovanni Tinè (Member, IEEE) received the M.S. degree in electronic engineering and the Ph.D. degree in electronics, computer science, and telecommunications engineering from the University of Palermo, Palermo, Italy, in 1990 and 1994, respectively.

He is currently a Researcher with the Institute of Marine Engineering, Italian National Research Council, Palermo. His current research interests include electromagnetic compatibility, power-line communications, and smart grids.